A Non local Variational Formulation for the Optimization of Tone Mapping Operators

Praveen Cyriac, Thomas Batard, Marcelo Bertalmío

A NON LOCAL VARIATIONAL FORMULATION FOR THE OPTIMIZATION OF TONE MAPPING OPERATORS *

PRAVEEN CYRIAC , THOMAS BATARD , AND MARCELO BERTALMÍO †

Abstract. Due to technical limitations, common display devices can only reproduce images having a low range of intensity values (dynamic range). As a consequence, the dynamic range of images encoding real world scenes, which is large, has to be compressed in order for them to be reproduced on a common display, and this technique is called tone mapping. A good tone mapping operator should make the image on the screen be perceived as the original scene, but the main issue is that the quality of a tone mapping operator may vary greatly depending on the image attributes considered, and this might influence the way to design the tone mapping operator. In this paper, we address this issue by showing that, for a large class of metrics comparing perceptual attributes between images, it is possible to improve any tone mapping operator with respect to these metrics. The key idea of our approach is first to consider a given metric as a non local operator, then to formulate the problem of making the output image perceptually closer to the real world scene with respect to this metric as a minimization problem. Experiments on a particular metric tested with different tone mapping operators and images validate our approach.

Key words. Tone mapping, non local variational problem, perceptual distance, just noticeable difference

1. Introduction.

1.1. On tone mapping operators.

1.1.1. The tone mapping challenge. The vast range of light intensities of the real world span many orders of magnitude. Even though the Dynamic Range (DR) of the Human Visual System (HVS) is only 3-4 orders of magnitude, nonetheless it is capable to handle intensities from about 10^{-6} to 10^{8} cd/m^2 [21], due to the fact that it continuously adjusts to the light in any viewed scene. As the DR of most cameras is only 2-3 orders of magnitude, they tend to fail in capturing the details and contrast that we perceive with the naked eye.

The most popular approach to capture the real world luminance is to create High Dynamic Range (HDR) images through the fusion of multiple Low Dynamic Range (LDR) images generated by a standard camera shooting the scene with varying exposure time [6]. However, HDR images can not be directly reproduced on common displays since their ranges usually span only two orders of magnitude, meaning that they can only reproduce LDR images.

Hence, a range compression of HDR images has to be performed in order for them to be reproduced on common displays, and this technique is called tone mapping. In particular, a good tone mapping operator (TMO) should produce in anyone watching the display a perception of details as close as possible to the one he/she would have had by observing the original scene directly [27].

1.1.2. Overview of tone mapping operators. Tumblin and Rushmeir [25] formally introduced the problem of tone mapping to the computer graphics field. The TMO they propose aims at transforming the real world luminance into the luminance generated by the display device. Since then, many TMOs have been proposed, and can be classified as global or local approaches.

*This work was supported by European Research Council, Starting Grant ref. 306337. Reduced version of this work appeared as a conference paper in [4].

†Department of Information and Communication Technologies, University Pompeu Fabra, Barcelona, Spain(praveen.cyriac@upf.edu, thomas.batard@upf.edu, marcelo.bertalmio@upf.edu).

Most of global TMOs consist in applying a compression curve to the image levels, based on psychovisual laws. Besides Tumblin and Rushmeir [25] who use Stevens' law, the Naka-Rushton formula is used in ([21],[23],[13]), Ferwerda's model in [12], and Weber-Fechner's law in ([2],[27]) to name a few. In particular, Reinhard et al. [23] developed a TMO based on the idea that tone mapping is similar to the adaptation process in the HVS, and used a modification of the Naka-Rushton equation. Drago et al. [7] introduced an adaptive logarithmic curve using a collection of logarithmic functions ranging from log_2 to log_{10}, the choice of the logarithm base depending on the luminance values. Mantiuk et al. [18] developed a piece-wise linear tone curve to achieve DR compression, whose parameters are chosen so as to minimize the difference between the estimated response of the HVS for the resultant image and the original image. Global TMOs are in general very fast and do not introduce halos or artifacts, but tend to produce low contrast images.

Local TMOs achieve DR compression by modifying each pixel based on its neighborhood. Even though they are computationally more expensive than global approaches, they produce higher contrast images. However they have the tendency to produce artefacts and halos [8][10][16].

More recently, Ferradans et al. [11] proposed a two stage TMO combining both approaches. The first stage is a global tone mapping method that implements visual adaptation by combining the Naka-Rushton equation and Weber-Fechner's law. The second stage performs local contrast enhancement, based on a variational model inspired by colour vision phenomenology.

1.1.3. Evaluation of tone mapping operators. The most straightforward way to evaluate a TMO is to perform a subjective evaluation, where observers rate the tone mapped image by comparing with the reference HDR image displayed on a HDR screen [14], or they simply evaluate the tone mapped image by itself, without any reference [29]. Subjects are asked to consider the image attributes such as brightness, contrast, colors, and naturalness, as well as overall quality. But subjective evaluation is limited in many ways: firstly, it is often time consuming and expensive; secondly, it is difficult to incorporate it in the design of tone mapping algorithms. This points out the importance of objective evaluation of TMOs.

An accurate objective evaluation should mimic the subjective evaluation described above, so it requires the use of a perceptual metric between images of different dynamic range. An objective tone mapping evaluation tool has been proposed by Smith et al. [24], based on the measure of suprathreshold contrast distortion between the source HDR image and its tone mapped LDR version. However, the contrast measure is local, meaning that its sensitivity is limited to high frequency details. More recently, Aydin et al. [3] proposed a dynamic range independent metric (DRIM) whose contrast measure is not limited to the values of neighboring pixels. Moreover, the metric predicts three type of distortions at each pixel between the two images it compares: loss of visible features, amplification of invisible features, and reversal of contrast polarity (see Sect. 3.1 for a more detailed description of the metric DRIM).

1.2. Contribution. The quality of the TMO may vary greatly from one metric to another. For this reason, we propose in this paper a new approach for tone mapping that takes into account the metric that will be used for the evaluation. In such a way, we are able to improve existing TMO with respect to a given metric. The aim of this paper is two-fold:

1. We develop a general framework for reducing perceptual distance between images. Dealing with a generic perceptual metric met and images H, L_0 of any

dynamic range, our approach for reducing the perceptual distance between H and L_0 is to minimize functionals of the form

$$\arg\min_{L\in C^\infty(\Omega;[0,1])} \int_\Omega \Phi(met(L,H)(x))\,dx \tag{1.1}$$

where $\Phi\colon \mathbb{R}^n \longrightarrow \mathbb{R}^+$, through gradient descent algorithms of initial condition L_0. Then the main task to perform the algorithm is to construct a discrete approximation of the functional derivative

$$\frac{\partial met(L,H)(x)}{\partial L(y)} \tag{1.2}$$

Our purpose is to introduce perceptual uniformity since the discretization is made on intensity values and not spatial coordinates. More precisely, we make use of the concept of Just Noticeable Difference (JND).

2. We apply the general framework described in (1.1). to the optimization of TMOs assuming that H is a HDR image, the initial condition L_0 is a tone mapped version of H and the metric met compares images of different dynamic range. In this paper, we illustrate our approach with the metric DRIM [3]. More precisely, we consider the following particular cases of (1.1)

$$\arg\min_{L\in LDR(\Omega)} \int_\Omega \|DRIM(L,H)(x)\|_k\,dx \tag{1.3}$$

where $k \in \mathbb{R}^*$. We evaluate our method by comparing the initial distance and distortions map (see details in Sect.3.1) with the ones of the output.

This paper is organized as follows. In Sect. 2, we formulate the problem of reducing a perceptual distance between images as a non local variational problem of the form (1.1). We first give the expression of the gradient of the functional to minimize in the continuous setting. Then, we provide an insight into the expression of the discrete gradient. In Sect. 3, we present an application of this general formulation to TMO optimization. We first describe the perceptual distance DRIM used for evaluating TMO. Then, we give explicit expressions of the discrete gradients of the functionals (1.3) from a discrete approximation of the functional derivative (1.2) relatively to the metric DRIM. We test the corresponding gradient descent algorithms on several tone mapped images in order to validate our approach.

2. Reducing the perceptual distance between two images.

2.1. Perceptual distance as a non local operator. Many tasks in image processing and computer vision require a validation by comparing the result with the original data, e.g. optical flow estimation, image denoising, tone mapping. Whereas measures based on pixel-wise comparisons (e.g. MSE, SNR, PSNR) are suitable to evaluate image denoising and optical flow estimation algorithms, they are not relevant to evaluate tone mapping since an accurate measure of the quality of a TMO should involve perceptual concepts, e.g. color sensation and detail visibility (contrast). This leads us to the following definitions.

Definition 2.1 (metric). *Let $L, H\colon \Omega \longrightarrow \mathbb{R}$ be two images. We call* ***metric*** *an operator* ***met*** *such that $met(L,H)$ is of the form $met(L,H)\colon \Omega \longrightarrow \mathbb{R}^n, n \geq 1$. We*

consider the functional partial derivatives of met, i.e.

$$\frac{\partial met(L,H)(x)}{\partial L(y)} := \lim_{\epsilon \to 0} \frac{met(L+\epsilon\delta_y, H)(x) - met(L,H)(x)}{\epsilon} \tag{2.1}$$

$$\frac{\partial met(L,H)(x)}{\partial H(y)} := \lim_{\epsilon \to 0} \frac{met(L, H+\epsilon\delta_y)(x) - met(L,H)(x)}{\epsilon} \tag{2.2}$$

where δ_y is the Dirac delta function concentrated at the point $y \in \Omega$.

We say that met is
(i) ***pixel-wise*** *if $\forall x, y \in \Omega, y \neq x$, the quantities (2.1), (2.2) vanish.*
(ii) ***non local*** *if $\forall x \in \Omega, \exists \mathcal{N}(x) \ni x, \mathcal{N}(x) \neq \{x\}, \exists y \notin \mathcal{N}(x)$ s.t. the quantities (2.1), (2.2) do not vanish.*

In this context, we can classify image quality measures into two categories. The set of pixel-wise metrics includes MSE, PSNR and SNR measures. Indeed, the terms $met(L+\epsilon\delta_y, H)(x) - met(L,H)(x)$ and $met(L, H+\epsilon\delta_y)(x) - met(L,H)(x)$ in formulae (2.1), (2.2) vanish for $y \neq x$ since such quantities only depend of the values $L(x)$ and $H(x)$. The second category gathers the metrics that are non local. This category contains the perceptual metrics since the perceptual difference at each pixel requires the knowledge of the intensity values on a large neighborhood of this pixel. This category can actually be divided into two sub-categories: the set of metrics that compare images of same dynamic range (see e.g. [5] for LDR images, [15],[19] for HDR images, and [26] for images of any dynamic range), and the set of metrics comparing images of different dynamic range (see e.g. [24]). The metric DRIM [3] belongs to both sub-categories since it is independent of the dynamic range of the images it compares.

Definition 2.2 (distance). *A* ***distance*** *associated to the metric* ***met*** *is an energy E of the form*

$$E\colon (L,H) \longmapsto \int_\Omega \Phi(met(L,H)(x))\, dx \tag{2.3}$$

for some map $\Phi\colon \mathbb{R}^n \longrightarrow \mathbb{R}^+$.

We say that the distance E is pixel-wise, resp. non local if the associated metric is pixel-wise, resp. non local.

2.2. Gradient descent algorithm in the continuous setting. From now on, we treat the problem of minimizing the distance E between two images. Given an image H, we consider the following variational problem

$$\underset{L \in C^\infty(\Omega;[0,1])}{\arg\min} \; E(L,H) \tag{2.4}$$

Proposition 2.3. *Assuming that met is continuous, bounded, and Φ is continuous, the variational problem (2.4) has a solution.*

Proof. Under the assumption of the Proposition, the energy E is bounded since the domain Ω of an image is a compact subset of $\mathbb{R}^2$. Moreover, the set $C^\infty(\Omega;[0,1])$ being closed, we deduce that there exists a function $L^* \in C^\infty(\Omega;[0,1])$ (not necessarily unique) solution of the variational problem (2.4). □

PROPOSITION 2.4. *Assuming that met and Φ are differentiable, the functions L which are critical points of the energy*

$$E_H \colon L \longmapsto E(L,H) \tag{2.5}$$

satisfy

$$\int_\Omega \delta\Phi\left(met(L,H)(x); \frac{\delta met(L,H)(x)}{\delta L(y)}\right) dx = 0 \qquad \forall y \in \Omega$$

Proof. The functional E_H being differentiable on the whole set $C^\infty(\Omega;[0,1])$, its critical points are the functions L where its gradient ∇E_H vanishes.

Let $\psi \colon \Omega \longrightarrow \mathbb{R}$ be a compact support function. We compute the differential δE of the energy E at a function L in the direction ψ. We have

$$\begin{aligned}
\delta E_H(L;\psi) &= \delta\, E((L,H);(\psi,0)) \\
&= \int_\Omega \delta\ (\Phi \circ met)\,((L,H);(\psi,0))(x)\, dx \\
&= \int_\Omega \delta\, \Phi\,(met(L,H)(x); \delta\, met\,((L,H);(\psi,0))(x))\, dx
\end{aligned}$$

The term

$$\delta\, met\,((L,H);(\psi,0))(x)$$

is the differential of the functional $L \longmapsto met(L,H)(x)$ in the direction ψ, and is defined by

$$\delta met\,((L,H);(\psi,0))(x) = \int_\Omega \frac{\partial met(L,H)(x)}{\partial L(y)} \psi(y)\, dy \tag{2.6}$$

where the definition of the term

$$\frac{\partial met(L,H)(x)}{\partial L(y)}$$

is given in formula (2.1). Finally we have

$$\delta E_H(L;\psi) = \int_{\Omega^2} \delta\Phi\left(met(L,H)(x); \frac{\delta met(L,H)(x)}{\delta L(y)}\right) \psi(y)\, dx\, dy$$

At last, as ψ has compact support, $\delta E_H(L;\psi) = 0 \Longrightarrow$

$$\int_\Omega \delta\Phi\left(met(L,H)(x); \frac{\delta met(L,H)(x)}{\delta L(y)}\right) dx = 0 \qquad \forall y \in \Omega \tag{2.7}$$

□

The gradient of the functional E_H at the function L is the map

$$\nabla E_H(L) \colon y \longmapsto \int_\Omega \delta\Phi\left(met(L,H)(x); \frac{\delta met(L,H)(x)}{\delta L(y)}\right) dx \tag{2.8}$$

Due to the lack of mathematical properties of the non local operators *met* encoding perceptual metrics, it is hard to establish accurate numerical schemes for reaching solutions of the variational problems (2.4). For this reason, we deal in this paper with the gradient descent algorithm, since it is applicable to a large class of functionals. As the variational problems (2.4) are minimization problems under constraints, we adopt a projected gradient descent approach

$$L_{n+1} = P(L_n - \alpha_n \nabla E_H(L_n)), \quad L_{|n=0} = L_0 \tag{2.9}$$

where P denotes the projection onto the space $C^\infty(\Omega; [0,1])$.
We would like to point out that the gradient descent (2.9) might converge towards critical points L_* that are not global minima. However, we have $E_H(L_*) < E_H(L_0)$ meaning that our method does reduce the perceptual distance of L_0 with respect to H.

2.3. The discrete gradient descent algorithm. The main task to compute a discrete approximation of the gradient (2.8) is to compute accurate discrete approximations of the functional derivative

$$\frac{\partial met(L,H)(x)}{\partial L(y)} := \lim_{\epsilon \to 0} \frac{met(L+\epsilon\delta_y, H)(x) - met(L,H)(x)}{\epsilon}$$

where δ_y is the Dirac delta function concentrated at the point $y \in \Omega$.

Our proposal is to make use of central differences of the form

$$\frac{\partial met^D(L,H)(a,b)}{\partial L(i,j)} := \frac{met(L+\epsilon_1\,\delta_{(i,j)}, H)(a,b) - met(L-\epsilon_2\,\delta_{(i,j)}, H)(a,b)}{2\,d(L+\epsilon_1\,\delta_{(i,j)}, L-\epsilon_2\,\delta_{(i,j)})} \tag{2.10}$$

for some well-chosen ϵ_1, ϵ_2, and where $d(L+\epsilon_1\,\delta_{(i,j)}, L-\epsilon_2\,\delta_{(i,j)})$ measures a difference between the two images $L+\epsilon_1\,\delta_{(i,j)}$ and $L-\epsilon_2\,\delta_{(i,j)}$. A straightforward choice would be to impose ϵ_1, ϵ_2 to be constant with respect to the intensity values of L and the denominator to be $\epsilon_1 + \epsilon_2$, however we claim that perceptual uniformity should be involved since the increments are done on the intensity values.

2.3.1. On perceptual uniformity. In the domain of psychophysics, the Just Noticeable Difference (JND) is the smallest difference ΔI in the intensity of a stimulus at which a human is able to perceive a difference between a uniform intensity I and a superimposed intensity $I + \Delta I$.

The Weber's law, named after the German physician E.H.Weber, relates the JND with the intensity of the stimulus according to the formula

$$\frac{\text{JND}}{I} = k \tag{2.11}$$

for some constant $k > 0$. Note that k varies with the natur of the stimulus. Regarding perception, visual experiments conducted later on by others showed that the Weber's law holds for a large range of light intensity I. However, it is a fact that the relation does not hold for low-intensity values.

The **luminance**, denoted by Y, is a measure of the perceived light and is defined as the radiance (light intensity reaching the retina) weighted by spectral sensitivity functions. However the space Y is not perceptually uniform in the sense that the

difference between two luminance values is not proportional to the difference of light intensity observed. In 1976, the CIE introduced **lightness** as the quantity

$$L^* = \begin{cases} 903.3\,\dfrac{Y}{Y_n} & \text{if} \quad \dfrac{Y}{Y_n} \leq 0.008856 \\ \\ 116\left(\dfrac{Y}{Y_n}\right)^{1/3} - 16 & \text{if} \quad \dfrac{Y}{Y_n} > 0.008856 \end{cases} \tag{2.12}$$

where Y_n is the highest luminance value of the scene. The quantity Y/Y_n is called **relative luminance**. **The space $\mathbf{L}^*$ is perceptually uniform**, and has a range of 0 to 100. In particular, a difference of 1 in L^* approximates pretty well 1 JND. Note that when scaled to the range 0...1, L^* can be approximated by the 0.4-power of the relative luminance, i.e. we have the relation

$$0.01L^* \simeq \left(\frac{Y}{Y_n}\right)^{0.4} \tag{2.13}$$

When shooting a scene, a digital camera captures the light intensity from which it encodes R, G, B values. Standard digital cameras also perform **gamma correction**:

$$R' = R^{\frac{1}{\gamma}} \qquad G' = G^{\frac{1}{\gamma}} \qquad B' = B^{\frac{1}{\gamma}} \tag{2.14}$$

Assuming that these values are encoded in the sRGB color space (which is the standard color space used in the broadcast and computer industries), γ is approximately 2.2. Gamma correction was introduced to compensate the non-linearity of the CRT displays. Even though CRTs have become obsolete, gamma correction is still used for efficient coding, i.e. to allocate more bits to encode the low intensity regions (where the HVS is more sensitive to changes) and less bits for bright regions. Then the relative luminance Y/Y_n perceived at a monitor displaying the image is given by

$$\frac{Y}{Y_n} \simeq 0.2126\,R'^{\gamma} + 0.7152\,G'^{\gamma} + 0.0722\,B'^{\gamma} \tag{2.15}$$

We refer to the book of Poynton [22] for detailed explanations about all these concepts. From formulae (2.15) and (2.13), and the fact that the term Y_n equals 1 when the colors are encoded in the sRGB color space, we end up with the formula

$$L^* \simeq (0.2126\,R'^{\gamma} + 0.7152\,G'^{\gamma} + 0.0722\,B'^{\gamma})^{0.4} \tag{2.16}$$

(assuming that the lightness is normalized to the range [0,1]).

Finally, from formula (2.16) and using the perceptual uniformity of the lightness L^*, we can express the JND for light intensities of a color image of components (R', G', B') perceived at the screen.

2.3.2. Expression of the discrete gradient. Based on the analysis done in Sect. 2.3.1., we argue that the increments ϵ_1, ϵ_2 as well as the measure d in formula (2.10) should be related to the JND. However, we have to face two issues:

(i) The JND is determined on a uniform background whereas expression (2.10) deals with image pixels.
(ii) Perceptual metrics do not necessarily compare images based on their lightness values, i.e. they are not defined on perceptually uniform spaces.

In order that the computation of the JND at an image pixel makes more sense, our proposal is to use at some point a smoothed version of the image L

$$\tilde{L} := L * G_\sigma \tag{2.17}$$

where G_σ is the Gaussian kernel associated to some variance σ. Indeed, convolving an image with a Gaussian kernel reduces its variations, making the smoothed image be locally closer to a uniform patch than the original image.

In order to overcome (ii), we have to take into account the specificity of the metric involved. In particular, the metric DRIM that we will use in Sect. 3 for tone mapping takes into account the luminance perceived at a display device, meaning that we will have to make use at some point of the formula (2.16).

In any case, the expression of the discrete approximation of the gradient (2.8) is of the form

$$\nabla^D E_H(L)\colon (i,j) \longmapsto \sum_{a,b} \delta\Phi\left(met(L,H)(a,b); \frac{\partial\, met^D(L,H)(a,b)}{\partial\, L(i,j)}\right) \tag{2.18}$$

and the projected gradient descent approach is

$$L_{n+1} = P^D(L_n - \alpha_n \nabla^D E_H(L_n))$$

where P^D denotes the projection onto the set of matrices of size Ω with values in the range $[0,1]$.

3. Application to the Optimization of Tone Mapping Operators.

3.1. Dynamic range independent perceptual distances. As mentioned above, the metric DRIM of Aydin et al. [3] compares in a perceptual manner images of any dynamic range. It aims at predicting details (contrast) changes between two images.

The purpose of this metric is to consider the perception that a viewer would have of both images relying on psychophysical data, and to estimate at each pixel the probabilities that distortions between the two images appear. More precisely, the metric first predicts whether the contrast is visible or not in each image, using the detection module HDR-VDP [15], from which two perceptually normalized response maps are produced, one for each image. The Cortex transform [28], with the modification from Daly [5], splits each response into several bands of different orientation and spatial bandwidth, then the metric estimates three types of distortions between the two images for each band and combine them. The outputs of the metric are the probabilities for each distortion to be detected at any band. The distortions considered are the following: Loss of Visible Contrast (LVC), meaning that contrast is visible in one image (called the reference image) and not in the second one (called test image); Amplification of Invisible Contrast (AIC), when details that were not in the reference image appear in the test image; and contrast reversal (INV), meaning that contrast is visible in both reference and test images but with different polarity. Note that for applications to tone mapping evaluation, the reference image is the luminance map of an HDR image and the test image is the luminance map of its LDR tone mapped version.

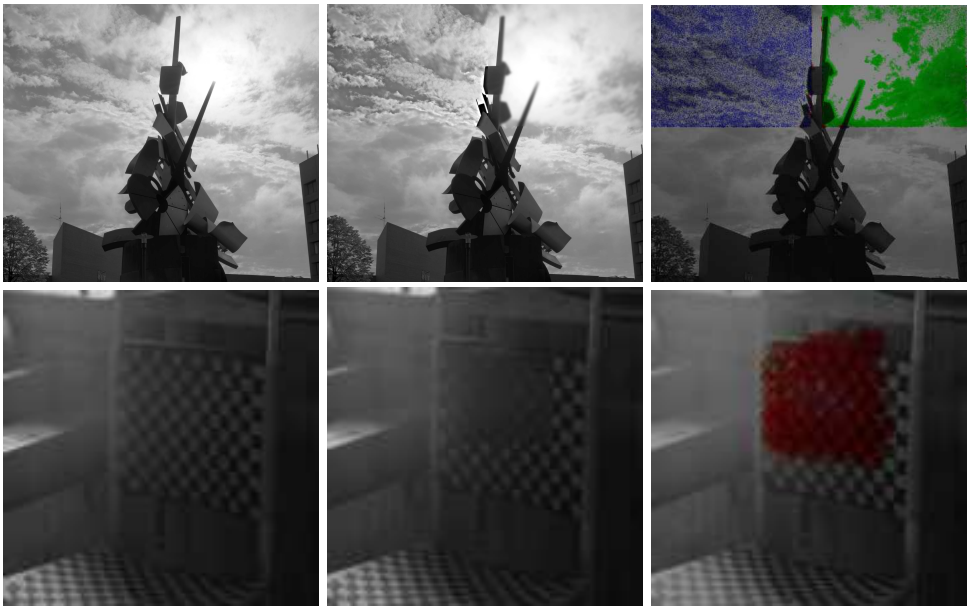

FIG. 3.1. *Distortion map illustration. Left: reference images. Middle: test images. Right: distortion maps.*

The metric also provides a distortion map to encode pixel-wise distortions with the following color code: green hue represents LVC, blue hue stands for AIC and red hue indicates INV, the saturation encoding the magnitude of the corresponding distortion, whereas the intensity corresponds to the intensity of the reference image (up to rounding). At each pixel, the maximum of the three distortions is computed, and the corresponding color is displayed. If the maximum is lower than 0.5, then the saturation is set to 0.

These three types of distortions estimated by the metric DRIM are illustrated on Fig. 3.1. On the left column, we show two LDR grey-level images. We apply some filters to these images in order to create distortions. To the reference image located in the top row, we apply a Gaussian smoothing on its top-right part and unsharp masking on its top-left part in order to obtain respectively a contrast reduction and a contrast enhancement. To the reference image located in the bottom row, we apply some contrast reversal technique on the pattern in the chair. The images resulting of these filters are shown in the middle column. Then, we compute the metric DRIM where the reference images are the original images on the left column and the test images are their distorted versions in the middle column. The distortion maps, shown in the right column, are coherent with the artificial distortions we created.

As the output of the metric DRIM encode at each pixel the probabilities of detecting the distortions LVC,AIC,INV between two images, we reinterpret the metric DRIM as follows.

DEFINITION 3.1 (Dynamic range independent perceptual metric). *Let* $L, H : \Omega \longrightarrow \mathbb{R}$ *be two images of any dynamic ranges, the perceptual metric DRIM between* L *and*

H is the map

$$DRIM(L,H)\colon \begin{array}{ccc} \Omega & \longrightarrow & [0,1]^3 \\ x & \longmapsto & (LVC(L,H)(x), AIC(L,H)(x), INV(L,H)(x)) \end{array} \tag{3.1}$$

From the perceptual metric (3.1) we define a set of perceptual distances between images of any dynamic range.

DEFINITION 3.2 (Dynamic range independent perceptual distances). *Let $k \in \mathbb{R}^*$, the perceptual distance $E_k(L,H)$ between L and H is*

$$E_k(L,H) \colon = \|DRIM(L,H)\|_{L_k} \tag{3.2}$$

In others words, we have

$$E_k(L,H) = \int_\Omega (LVC^{\,k}(L,H)(x) + AIC^{\,k}(L,H)(x) + INV^{\,k}(L,H)(x))^{1/k}\ dx \tag{3.3}$$

3.2. Reducing the perceptual distance between an HDR image and its tone mapped version. Given an HDR image H, we aim at constructing the LDR image L minimizing the perceptual distance E_k with H.

3.2.1. Gradient descent algorithm in the continuous setting. Let four numbers a_1, a_2, b_1, b_2 with $0 \leq a_1 < a_2 < b_2 < b_1 \leq 1$. In this paper, we define the functional spaces $LDR(\Omega)$ and $HDR(\Omega)$ as follows

$$HDR(\Omega) = \{f \in C^\infty(\Omega; [a_1, b_1])\} \tag{3.4}$$

$$LDR(\Omega) = \{f \in C^\infty(\Omega; [a_2, b_2])\} \tag{3.5}$$

In particular, we have $LDR(\Omega) \subset HDR(\Omega)$.

PROPOSITION 3.3. *Let H be an HDR image. Assuming that the metric DRIM of Definition 3.1. is continuous, the variational problem*

$$\underset{L \in LDR(\Omega)}{\arg\min}\ E_k(L,H) \tag{3.6}$$

has a solution.

Proof. Each distortion being in the range $[0,1]$, the L_k norms being continuous, and the space $LDR(\Omega)$ being closed, Proposition 3.3 appears to be a particular case of Proposition 2.3. □

Note that the energy (3.2) is bounded by 0 and $3^{1/k}|\Omega|$.

PROPOSITION 3.4. *Assuming that H is non constant and the metric DRIM is differentiable on the space $LDR(\Omega)$, the critical points of the energy*

$$E_{k\,H}\colon L \longrightarrow E_k(L,H) \tag{3.7}$$

satisfy

(3.8)
$$\int_\Omega \frac{LVC(L,H)^{k-1}\frac{\partial LVC(L,H)}{\partial L(y)} + AIC(L,H)^{k-1}\frac{\partial AIC(L,H)}{\partial L(y)} + INV(L,H)^{k-1}\frac{\partial INV(L,H)}{\partial L(y)}}{(LVC(L,H)^k + AIC(L,H)^k + INV(L,H)^k)^{1-1/k}}\, d\Omega = 0$$

$\forall y \in \Omega$.

The proof of the Proposition relies upon the following postulate: **the metric DRIM only vanishes when the inputs are two identical constant images.** This postulate is based on many experiments that we have run.

Proof. The energy E_{kH} is differentiable on the whole set $LDR(\Omega)$ since the metric DRIM does not vanish for non constant images (postulate). Then, according to Prop. 2.4, the critical points of (3.7) satisfy

$$\int_\Omega \delta\| \, \|_k \left(DRIM(L,H)(x); \frac{\delta DRIM(L,H)(x)}{\delta L(y)} \right) dx = 0 \qquad \forall y \in \Omega \tag{3.9}$$

Finally, expression (3.8) follows from (3.9) and

$$\delta\| \, \|_k((u_1,u_2,u_3);(v_1,v_2,v_3)) = \frac{u_1^{k-1}v_1 + u_2^{k-1}v_2 + u_3^{k-1}v_3}{\|(u_1,u_2,u_3)\|_k{}^{k-1}}$$

□

The term $\nabla E_{kH}(L)\colon y \longmapsto$

(3.10)
$$\int_\Omega \frac{LVC(L,H)^{k-1}\frac{\partial LVC(L,H)}{\partial L(y)} + AIC(L,H)^{k-1}\frac{\partial AIC(L,H)}{\partial L(y)} + INV(L,H)^{k-1}\frac{\partial INV(L,H)}{\partial L(y)}}{(LVC(L,H)^k + AIC(L,H)^k + INV(L,H)^k)^{1-1/k}}\, d\Omega$$

is the gradient of the energy E_{kH} at the function L.

As already mentioned in Sect. 2.2, perceptual metrics like DRIM lack mathematical properties. Hence, to the best of our knowledge, there exists no scheme that would systematically converge towards the solutions of the variational problem (3.6). Then, our proposal is to make use of a projected gradient descent algorithm of the form

$$L_{n+1} = P(L_n - \alpha_n \nabla E_{kH}(L_n)), \quad L_0 = TMO(H) \tag{3.11}$$

where P denotes the projection onto the space $LDR(\Omega)$, and the initial condition L_0 is a tone mapped version of H. Even if the scheme (3.11) may converge towards local minima of the energy E_{kH} that are not global, it reduces the perceptual distance $E_{kH}(L_0)$ of the initial condition L_0 with H, which validates our approach for TMO optimization.

Actually, as the perceptual metric involved is the metric DRIM, the initial condition L_0 of the gradient descent (3.11) should be the light intensity provided by a screen when displaying the tone mapped image TMO(H). Denoting by R_0, G_0, B_0 the inverse gamma corrected (see Sect. 2.3.1) components of the tone mapped image TMO(H) in the sRGB color space, we transform TMO(H) into XYZ color coordinates

with the formula

$$\begin{pmatrix} X_0 \\ Y_0 \\ Z_0 \end{pmatrix} = \begin{pmatrix} 0.4124 & 0.3576 & 0.1805 \\ 0.2126 & 0.7152 & 0.0722 \\ 0.0193 & 0.1192 & 0.9502 \end{pmatrix} \begin{pmatrix} R_0 \\ G_0 \\ B_0 \end{pmatrix} \tag{3.12}$$

As mentioned in Sect. 2.3.1., the component Y_0 is an approximation of the light intensity perceived when displaying a color image on a monitor. We then apply the gradient descent algorithm (3.11) where the initial condition is Y_0. Denoting by Y_* the steady-state of the scheme (3.11), the final output of our algorithm dedicated to optimize TMOs is the color image of components (R_*, G_*, B_*) defined by

$$\begin{pmatrix} R_* \\ G_* \\ B_* \end{pmatrix} = \begin{pmatrix} 0.4124 & 0.3576 & 0.1805 \\ 0.2126 & 0.7152 & 0.0722 \\ 0.0193 & 0.1192 & 0.9502 \end{pmatrix}^{-1} \begin{pmatrix} X_0 \\ Y_* \\ Z_0 \end{pmatrix}$$

3.2.2. The discrete gradient descent algorithm. The discrete approximation of the scheme (3.11) is of the form

$$L_{n+1} = P^D(L_n - \alpha_n \nabla^D E_{kH}(L_n)), \quad L_0 = Y_0 \tag{3.13}$$

where $\nabla^D E_{kH}$ is a discrete approximation of the gradient (3.10), and P^D denotes the projection onto the set of [0,1]-valued matrices. In what follows, we detail the construction of $\nabla^D E_{kH}$.

In the discrete case, we replace the gradient (3.10) by $\nabla^D E_{kH}(L)\colon (i,j) \longmapsto$

$$\sum \frac{LVC(L,H)^{k-1} \frac{\partial LVC^D(L,H)}{\partial L(i,j)} + AIC(L,H)^{k-1} \frac{\partial AIC^D(L,H)}{\partial L(i,j)} + INV(L,H)^{k-1} \frac{\partial INV^D(L,H)}{\partial L(i,j)}}{(LVC(L,H)^k + AIC(L,H)^k + INV(L,H)^k)^{1-1/k}} \tag{3.14}$$

Following Sect. 2.3, we compute a discrete approximation of the functional derivative of the metric $DRIM$ as

$$\frac{\partial DRIM^D(L,H)(a,b)}{\partial L(i,j)} := \frac{DRIM(L + \epsilon_1 \, \delta_{(i,j)}, H)(a,b) - DRIM(L - \epsilon_2 \, \delta_{(i,j)}, H)(a,b)}{2d(L + \epsilon_1 \, \delta_{(i,j)}, L - \epsilon_2 \, \delta_{(i,j)})} \tag{3.15}$$

for some well-chosen $\epsilon_1, \epsilon_2, d$ determined in the following paragraph, and from which follows the functional derivatives

$$\frac{\partial LVC^D(L,H)(a,b)}{\partial L(i,j)} \qquad \frac{\partial AIC^D(L,H)(a,b)}{\partial L(i,j)} \qquad \frac{\partial INV^D(L,H)(a,b)}{\partial L(i,j)}$$

Computation of $\epsilon_1, \epsilon_2, d$. As mentioned in Sect. 2.3.2, the key idea to compute (3.15) is to approximate the JND in the luminance space. We can express the JND for the luminance L (denoted by Y in Sect. 2.3.1) perceived at the screen using the formula (2.16) and (2.17) as follows. Let $(i,j) \in \Omega$, we have

$$\Delta \tilde{L}^{0.4}(i,j) = 0.01 \tag{3.16}$$

where $\tilde{L}$ is a smoothed version of L (see Sect. 2.3). Then, solving the equation

$$(\tilde{L}(i,j)+\epsilon_1)^{0.4} - \tilde{L}^{0.4}(i,j) = 0.01 \tag{3.17}$$

yields

$$\epsilon_1 = (\tilde{L}^{0.4}(i,j)+0.01)^{2.5} - \tilde{L}(i,j) \tag{3.18}$$

In the same manner, solving the equation

$$\tilde{L}^{0.4}(i,j) - (\tilde{L}(i,j)-\epsilon_2)^{0.4} = 0.01 \tag{3.19}$$

yields

$$\epsilon_2 = \tilde{L}(i,j) - (\tilde{L}^{0.4}(i,j)-0.01)^{2.5} \tag{3.20}$$

However, defining ϵ_1, ϵ_2 as in (3.18), (3.20) might yield an extra issue:

(iii) $L(i,j)+\epsilon_1 > 1$ or $L(i,j)-\epsilon_2 < 0$. In such a case, the quantity (2.10) would not be defined.

We then relax the perceptual uniformity paradigm in order to stay in the range $[0,1]$ of the image L. We end up with the following two extensions of equations (3.17) and (3.19)

$$(\tilde{L}(i,j)+\epsilon_1)^{0.4} - \tilde{L}^{0.4}(i,j) = \min(0.01, 1-\tilde{L}^{0.4}(i,j)) \tag{3.21}$$

$$\tilde{L}^{0.4}(i,j) - (\tilde{L}(i,j)-\epsilon_2)^{0.4} = \min(0.01, \tilde{L}^{0.4}(i,j)) \tag{3.22}$$

whose solutions are

$$\epsilon_1 \colon = (\tilde{L}^{0.4}(i,j) + \min(0.01, 1-\tilde{L}^{0.4}(i,j)))^{2.5} - \tilde{L}(i,j) \tag{3.23}$$

$$\epsilon_2 \colon = \tilde{L}(i,j) - (\tilde{L}^{0.4}(i,j) - \min(0.01, \tilde{L}^{0.4}(i,j)))^{2.5} \tag{3.24}$$

Hence, $L+\epsilon_1\delta_{i,j}$ never exceeds 1 since $\tilde{L} \leq L$ by construction. For the same reason, $L-\epsilon_2\delta_{i,j}$ never gets negative.
We then set

$$d = min(0.01, 1-\tilde{L}^{0.4}(i,j)) + min(0.01, \tilde{L}^{0.4}(i,j)) \tag{3.25}$$

3.2.3. Preprocessing. To increase the chance that the gradient descent algorithm (3.13) does not stop at a local minimum of the energy E_{k_H} too close to the initial condition L_0, we apply a preprocessing on L_0 in order to get an initial condition L_{new} of the algorithm (3.13) that is closer (in terms of perceptual distance) to H than L_0. The method we propose relies on the intuition that high values of LVC might be reduced by application of local sharpening whereas high values of AIC might be reduced by local Gaussian blurring. Hence we perform local Gaussian blurring and unsharp masking [1] to L_0 depending on the values of the function $LVC(L_0,H) - AIC(L_0,H)$.

Denoting by L_{smooth} a blurred version of L_0 and defining L_{sharp} as

$$L_{sharp} = L_0 + \alpha\,(L_0 - L_{smooth}) \tag{3.26}$$

for some constant α, we define the image L_{new} as

$$L_{new}(i,j) = \begin{cases} L_{sharp}(i,j) & \text{if} \quad LVC(L_0,H) - AIC(L_0,H)(i,j) > 0 \\ (1-\beta)L_0(i,j) + \beta L_{smooth}(i,j) & \text{if} \quad LVC(L_0,H) - AIC(L_0,H)(i,j) < 0 \end{cases} \tag{3.27}$$

Experiments on different tone mapped images described in the next Section show that the distance with H is indeed reduced as well as the errors in the distortion map.

3.2.4. Numerical scheme. We summarize in this Section the different steps of our algorithm.

1. Let H be an HDR image and L_0 be a tone mapped version of H. As the metric DRIM only takes into account the luminance information of the input images, we first convert them into luminance maps: we apply the transformation (3.12) on the LDR image L_0 and extract the luminance channel Y_0, and use the function *pfs_read_luminance*[17] to extract the luminance information of H.
2. We perform the preprocessing described in Sect. 3.2.3 on the image Y_0 with the following parameters: the variance σ of the Gaussian smoothing kernel is set to 0.62, and the constants α, β are respectively 0.7 and 0.5. These values provide good results and have been fixed for all the experiments in this paper.
3. We apply the gradient descent algorithm (3.13) where the initial condition is the output of the preprocessing. We test different values for k and different domains for the summation in the expression of the discrete gradient operator (3.14). Indeed, because the variational problem we propose is non local, the gradient operator is an integral operator, meaning that its computation might be very time-consuming. In order to decrease the execution time of the algorithm, we adopt the following two approaches: we consider 50×50 neighborhoods, and make use of computers equipped with multiple cores to compute the gradient operator over the whole image domain. The algorithm stops when the energy does not decrease anymore, i.e. when we reach a local or global minimum.

The pseudo code of the gradient descent algorithm is given below.

while $E_{new} < E_{old}$ **do**
  for each pixel p **do**
  $L_n^+ = L_n + \epsilon_1 \delta_p$
  $L_n^- = L_n - \epsilon_2 \delta_p$, ▷ ϵ_1, ϵ_2 from (3.23) and (3.24)
  $(LVC^{+/-}, AIC^{+/-}, INV^{+/-}) = DRIM(L_n^{+/-}, H)$,
  $Diff_{type} = (type^+ - type^-)/d$, $type \in Type = \{LVC, AIC, INV\}$ ▷ d from (3.25)
  $gradient(p) = \sum_X (\sum_{Type} type^{k-1} \times Diff_{type}) / (\sum_{Type} type^k)^{1-1/k}$
  ▷ X is either 50×50 or full image domain
  end for
$L_{n+1} = P^D(L_n - \alpha_n \times gradient)$, ▷ α_n from line search strategy and P^D from (3.13)

$(LVC, AIC, INV) = DRIM(L_{n+1}, H)$
$E_{old} = E_{new}$
$E_{new} = \sum_X (LVC^k + AIC^k + INV^k)^{1/k}$
end while

4. The final output LDR color image is then obtained by combining the X_0 and Z_0 components of the initial tone mapped image L_0 with the output produced by the gradient descent algorithm.

3.3. Experiments. We test our algorithm dedicated to optimize TMOs on different HDR images taken from the MPI [20] and Fairchild [9] databases, and the TMOs of Ferradans et al. [11], Drago et al. [7], Reinhard et al. [23], and Mantiuk et al. [18].

The evaluation of our algorithm is two-fold: global and pixel-wise. As a pixel-wise measure, we compare the distortion maps (see details in Sect. 3.1) of the initial condition and output. As a global measure, we compare their averaged perceptual distance with H, making use of the following energy

$$E(L, H) = \frac{1}{|\Omega|} \sum_{(a,b)\in\Omega} \|DRIM(L, H)(a, b)\|_2 \tag{3.28}$$

The first experiment we propose consists in evaluating the preprocessing. In Fig. 3.2, we show the input tone mapped images, output color images of the preprocessing, as well as their distortion maps. We have applied the formula (3.27) to the luminance channel of tone mapped images obtained with the method of Ferradans et al.[11] (top row image) and Drago et al. [7] (bottom row image). The HDR source images are taken from the MPI database [20]. We observe that the LVC distortion has been reduced, whereas the INV distortion has increased a bit. As we can see in formula (3.27), the preprocessing is only devoted to reduce the LVC and AIC distortions, and does not take into account the INV distortion. Hence, some choices of the parameters α, β might yield an increase of the INV distortion. On Table 3.1, we present results of the preprocessing (amongst other results) tested on images of the Fairchild database [9] for the TMOs aforementioned. Note that the images have been rescaled to 200×200 pixels in order to speed up the gradient descent algorithm. Average results have been computed over 10 images of the dataset. The results confirm that the preprocessing reduces the perceptual distance with respect to the HDR source image.

In the second experiment, we evaluate the final output of our method described above for different perceptual distances (3.2) parametrized by $k \in \mathbb{R}^*$. Table 3.1 shows the distance (3.28) of the initial tone mapped images and output images with a given HDR image for the following values of the parameter $k : 0.8, 1, 1.2, 2, 5$ and 50. The summation for the computation of the gradient operator (3.14) has been done on 50×50 neighborhoods. The results show that, in most of the cases, $k = 0.8$ provides the minimum distance. We also observe that the distance tends to increase with the value k.

In the third experiment, we compare the output of the preprocessing stage with the final output of our method using 50×50 neighborhoods and parameter $k = 0.8$, as well as their distortions maps (see Fig 3.3). The HDR source is the image "Peck-Lake" from the Fairchild database, and the input tone mapped image is provided by the TMO of Drago et al. [7]. Its corresponding distortion map reveals a great loss

FIG. 3.2. *Evaluation of preprocessing stage for Ferradans et al.[11] (top row) and Drago et al. (bottom row) TMOs. From left to right: input tone mapped image, output of preprocessing stage, distortion map of the input, distortion map of the output.*

TABLE 3.1
Distance with different k values.

Image \ TMO		Drago et al.[7]	Reinhard et al.[23]	Mantiuk et al.[18]	Ferradans et al.[11]
AmikBeav DamPM1	Initial	0.726	0.744	0.763	0.745
	Preprocess	0.573	0.611	0.66	0.702
	Final (k = 0.8)	0.464	0.515	0.59	0.546
	Final (k = 1)	0.469	0.517	0.59	0.545
	Final (k = 1.2)	0.474	0.519	0.59	0.546
	Final (k = 2)	0.494	0.534	0.6	0.558
	Final (k = 5)	0.543	0.57	0.624	0.559
	Final (k = 50)	0.561	0.588	0.639	0.602
Barharbor Presun	Initial	0.662	0.665	0.533	0.561
	Preprocess	0.53	0.552	0.493	0.511
	Final (k = 0.8)	0.417	0.454	0.446	0.46
	Final (k = 1)	0.416	0.452	0.442	0.457
	Final (k = 1.2)	0.418	0.453	0.444	0.454
	Final (k = 2)	0.433	0.465	0.447	0.462
	Final (k = 5)	0.469	0.508	0.47	0.490
	Final (k = 50)	0.496	0.528	0.484	0.501
Average (10 images)	Initial	0.645	0.657	0.573	0.590
	Preprocess	0.527	0.575	0.515	0.536
	Final (k = 0.8)	0.417	0.460	0.457	0.460
	Final (k = 1)	0.420	0.461	0.457	0.460
	Final (k = 1.2)	0.426	0.464	0.457	0.462
	Final (k = 2)	0.442	0.476	0.467	0.471
	Final (k = 5)	0.475	0.511	0.481	0.494
	Final (k = 50)	0.490	0.529	0.497	0.511

of contrast (green patches). We observe that the preprocessing stage reduces such a distortion, and the gradient descent algorithm applied to the output of the preprocessing reduces it to even greater extent. These improvements are confirmed when computing the perceptual distances (3.28) at each stage with the HDR source image: initial (0.639), preprocessing (0.509), and final (0.389). There is a 39% reduction in distance in the final image compared to the initial tone mapped image. From this result and the ones shown in Table 3.1 we can claim that applying the gradient de-

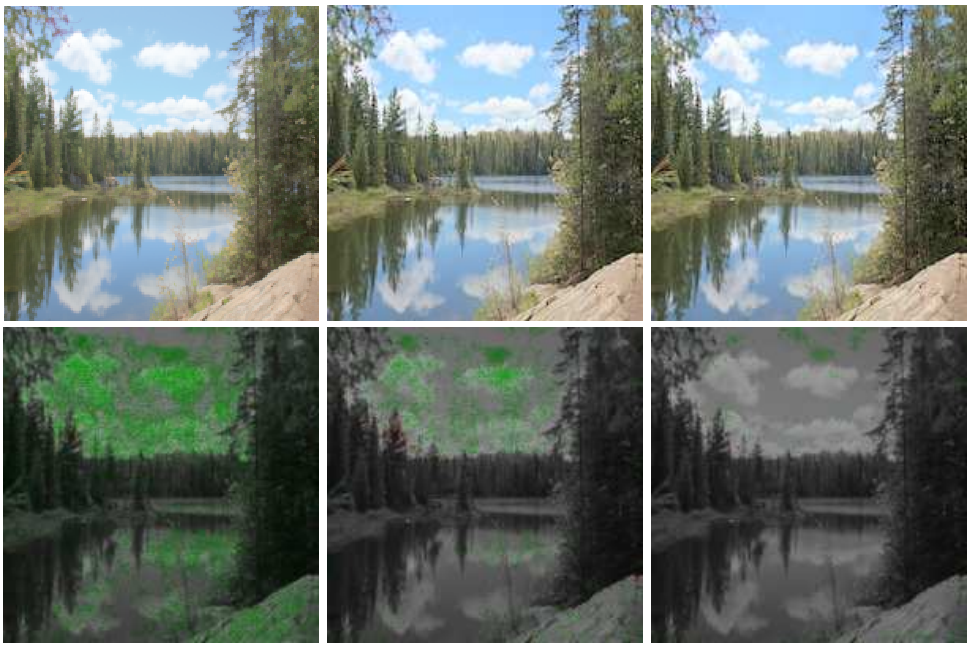

FIG. 3.3. *Comparison between the output of preprocessing stage and the final stage. Top left: input tone mapped image of Drago et al.[7]. Top middle: output of preprocessing stage. Top right: final output with* $k = 0.8$. *Bottom row: corresponding distortion maps.*

scent algorithm to the output of the preprocessing provides much better results than applying only the preprocessing.

At last, we analyze the impact of modifying the neighborhood size used for the summation in the expression of the gradient operator (3.14). We test our algorithm for 50×50 as well as 200×200 neighborhoods (the whole image domain). The parameter k has been set to 0.8, which is the value giving the best results in the case of 50×50 neighborhoods according to the second experiment. In Fig 3.4, we show the output color image obtained with the two neighborhood sizes along with their distortion maps. The HDR source is the image "BarHarborPresunrise" from the Fairchild database. The input tone mapped image is provided by the TMO of Reinhard et al. [23]. The distortion maps show that using the whole image domain substantially reduces the LVC distortion (less green patches appear in the distortion map), and reduces (in less proportion) the INV distortion (less red patches). In Fig 3.5, we show some results of our algorithm with a 200×200 neighborhood tested on the different TMOs mentioned above applied to the same HDR image. By a close observation of the output images, we can notice an enhancement of details of the initial tone mapped images which is confirmed by comparing the corresponding distortion maps (reduction of LVC distortion). Table 3.2 compares the distance between the final output images (using the aforementioned domains) with the HDR source image. We can see that the results obtained by using a 200×200 neighborhood have smaller error than the results achieved by using a 50×50 neighborhood, and this numerical behavior is consistent with the visual distortion maps presented in Fig 3.4.

4. Conclusion. Based on perceptual metrics that measure distortions between images, we propose in this paper a non local variational approach to minimize per-

FIG. 3.4. *Comparison between the final output with* 50×50 *and* 200×200 *neighborhoods. Top left: input tone mapped image of Reinhard et al. [23]. Top middle: final output with* 50×50 *neighborhood. Top right: final output with* 200×200 *neighborhood. Bottom row: corresponding distortion maps.*

TABLE 3.2
Distance at the final stage of our method with 50×50 *and* 200×200 *neighborhoods. Percentile improvement at each stage with respect to the original tone mapping result is given in brackets.*

TMO / Image		Drago et al.[7]	Reinhard et al.[23]	Mantiuk et al.[18]	Ferradans et al.[11]
AmikBeav DamPM1	Initial	0.726	0.744	0.763	0.745
	Preprocess	0.573 (21%)	0.611 (13%)	0.66 (14%)	0.702 (6%)
	Final (50×50)	0.464 (36%)	0.515 (31%)	0.59 (23%)	0.546 (27%)
	Final (200×200)	0.264 (64%)	0.356 (52%)	0.47 (38%)	0.388 (48%)
Barharbor Presun	Initial	0.662	0.665	0.533	0.561
	Preprocess	0.53 (20%)	0.552 (17%)	0.493 (7%)	0.511 (9%)
	Final (50×50)	0.417 (37%)	0.454 (32%)	0.446 (16%)	0.46 (18%)
	Final (200×200)	0.206 (69%)	0.248 (63%)	0.352 (34%)	0.34 (39%)

ceptual distances between two images of any DR. Then, we use this framework in the context of tone mapping by considering the perceptual metric DRIM [3]. The experiments show that our approach improves the TMOs tested in the sense that it reduces the perceptual distance of a tone mapped image with respect to its HDR source. Our method provides an average reduction of this distance by more than 25%.
Further work will be devoted to apply the proposed framework to contexts where minimization of a perceptual distance could also be useful. One such application may be to optimize gamut mapping methods by considering a perceptual metric that measures color distortions between images.

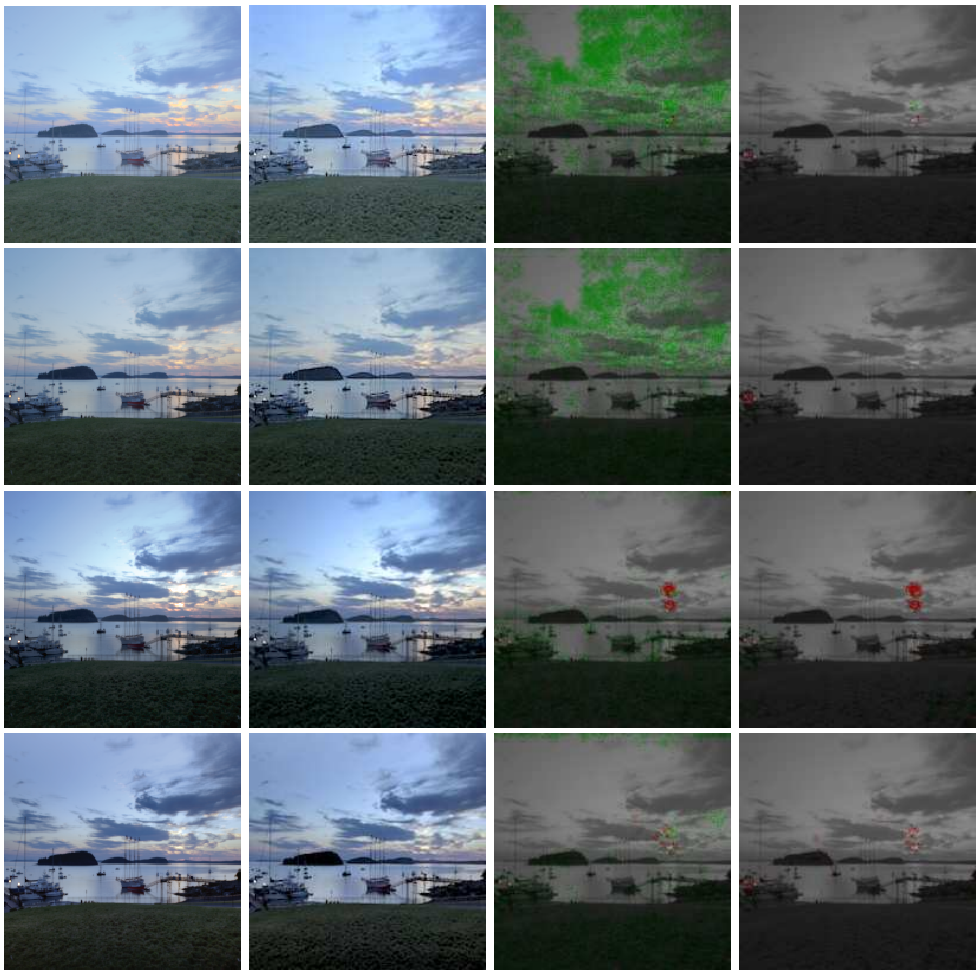

FIG. 3.5. *The final output. First column: input tone mapped images (TMOs from top to bottom: Drago et al.[7], Reinhard et al.[23], Mantiuk et al.[18], Ferradans et al. [11]). Second column: final output images with a* 200×200 *neighborhood. Third column: distortion maps of input tone mapped images. Fourth column: distortion maps of final outputs. See Table. 3.2 (image "BarharborPresun") for the corresponding distances.*

REFERENCES

[1] J.E. ADAMS, A.T. DEEVER, E.O. MORALES, B.H. PILLMAN, *Perceptually based image processing algorithm design. Perceptual Digital Imaging: Methods and Applications*, (2012), pp. 123-166.

[2] M. ASHIKHMIN,*A tone mapping algorithm for high contrast images*, Proc. Eurographics Workshop Rendering, (2002), pp. 1-11.

[3] T.O. AYDIN, R. MANTIUK, K. MYSZKOWSKI, AND H.-P. SEIDEL, *Dynamic range independent image quality assessment*, Proc. ACM SIGGRAPH 2008, (2008), pp. 1-10.

[4] P. CYRIAC, T. BATARD, AND M. BERTALMÍO, *A variational method for the optimization of tone mapping operators*, Proc. 6th Pacific-Rim Symposium on Image and Video Technology PSIVT 2013, R. Klette et al. Eds., LNCS 8333, (2014), pp. 505-516.

[5] S. DALY, *The visible differences predictor: an algorithm for the assessment of image fidelity*, Digital Images and Human Vision. MIT Press, A.B. Watson, Eds., (1993), pp. 179-206.

[6] P. E. DEBEVEC, J. MALIK, *Recovering high dynamic range radiance maps from photographs*,

ACM SIGGRAPH, (1997), pp. 369-378.
[7] F. DRAGO, K. MYSZKOWSKI, T. ANNEN, N. CHIBA,*Adaptive logarithmic mapping for displaying high contrast scenes*, Computer Graphics Forum, 22(3), (2003), pp. 419-426.
[8] F. DURAND, J. DORSEY, *Fast bilateral filtering for the display of high dynamic range images*, Proc. ACM SIGGRAPH, (2002), pp. 257-266.
[9] M.D. FAIRCHILD, *Color Appearance Models*, Wiley and Sons, 3rd Edition (2013).
[10] R. FATTAL, D. LISCHINSKI, M. WERMAN, *Gradient domain high dynamic range compression*, Proc. ACM SIGGRAPH, (2002), pp. 249-256.
[11] S. FERRADANS, M. BERTALMÍO, E. PROVENZI, AND V. CASELLES, *An analysis of visual adaptation and contrast perception for tone mapping*, IEEE Trans. Pattern Anal. Mach. Intell., 33(10) (2011), pp. 2002-2012.
[12] J. FERWERDA, S. PATTANAIK, P. SHIRLEY, D. GREENBERG, *A model of visual adaptation for realistic image syntesis*, Proc. ACM SIGGRAPH, (1996), pp. 249-258.
[13] J. KUANG, G. M. JOHNSON, M. FAIRCHILD, *iCAM06: A refined image appearance model for HDR image rendering*, J. Visual Comm. and Image Representation, 18, (2007), pp. 406-414 .
[14] P. LEDDA, A. CHALMERS, T. TROSCIANKO, H. SEETZEN, *Evaluation of tone mapping operators using high dynamic range display*, ACM SIGGRAPH, (2005), pp. 640-648.
[15] R. MANTIUK, S. DALY, K. MYSZKOWSKI, AND H.-P SEIDEL, *Predicting visible differences in high dynamic range images - model and its calibration*, Human Vision and Electronic Imaging X, SPIE Proceedings Serie, 5666, (2005), pp. 204-214.
[16] R. MANTIUK, K. MYSZKOWSKI, H.-P. SEIDEL, *A perceptual framework for contrast processing of high dynamic range images*, ACM Trans. Applied Perception, 3(3), (2006), pp. 286-308
[17] R. MANTIUK, G. KRAWCZYK, R. MANTIUK, H-P. SEIDEL, *High dynamic range imaging pipeline: perception-motivated representation of visual content.*, Human Vision and Electronic Imaging XII, SPIE Proceedings, 6492, (2007)
[18] R. MANTIUK, S. DALY, L. KEROFSKY, *Display adaptative tone mapping*, Proc. ACM SIGGRAPH, (2008), 68.
[19] R. MANTIUK, K.J. KIM, A.G. REMPEL, AND W. HEIDRICH, *HDR-VDP-2: A calibrated visual metric for visibility and quality predictions in all luminance conditions*, ACM Trans. Graphics, 30(4) (2011), 40.
[20] MPI database: `http://www.mpi-inf.mpg.de/resources/hdr/gallery.html`
[21] S. PATTANAIK, J. TUMBLIN, H. YEE, D. GREENBERG, *Time-dependent visual adaptation for fast realistic image display*, Proc. ACM SIGGRAPH, (2000), pp. 47-54.
[22] C. POYNTON, *Digital Videos and HDTV: Algorithms and Interfaces*, Morgan Kaufmann, (2003).
[23] E. REINHARD, K. DEVLIN, *Dynamic range reduction inspired by photoreceptor physiology*, IEEE Trans. Visualization and Computer Graphics, 11(1), (2005), pp. 13-24.
[24] K. SMITH, G. KRAWCZYK, K. MYSZKOWSKI, AND H.-P. SEIDEL, *Beyond tone mapping: enhanced depiction of tone mapped HDR images*, Computer Graphics Forum, 25(3) (2006), pp. 427-438.
[25] J. TUMBLIN, H. RUSHMEIR, *Tone reproduction for computer generated images*, IEEE Computer Graphics and Applications, 13(6), (1993), pp. 42-48.
[26] Z. WANG, AND A.C. BOVIK, *A universal image quality index*, IEEE Signal Processing Letters, 9(3), (2002), pp. 81-84.
[27] G. WARD, H. RUSHMEIER, C. PIATKO, *A visibility matching tone reproduction operator for high dynamic range scenes*, IEEE Trans. Visualization and Computer Graphics, 3(4), (1997), pp. 291-306
[28] A. WATSON, *The Cortex transform: rapid computation of simulated neural images*, Comp. Vision Graphics and Image Processing, 39, (1987), pp. 311-327.
[29] A. YOSHIDA, V. BLANZ, K. MYSZKOWSKI, H.P SEIDEL, *Perceptual evaluation of tone mapping operators with real-world scenes*, International Society for Optics and Photonics, (2005), pp. 192-203.